Southern Ocean freshening stalls deep ocean CO_2 release in a changing climate

Léa Olivier

lea.olivier@awi.de

Alfred Wegener Institute https://orcid.org/0000-0001-9014-0979

F. Alexander Haumann

Alfred Wegener Institute, Helmholtz Centre for Polar and Marine Research https://orcid.org/0000-0002-8218-977X

Article

Keywords:

Posted Date: May 16th, 2025

DOI: https://doi.org/10.21203/rs.3.rs-6530488/v1

Additional Declarations: There is **NO** Competing Interest.

Abstract

The Southern Ocean critically mitigates global surface warming by taking up a large portion of the carbon released to the climate system by human activities. While models suggest this carbon sink should weaken with human-induced climate change due to an increased upwelling of carbon-rich deep water, such a strong decline has not been observed over the past decades. Here, using circumpolar hydrographic observations, we reveal that the freshening of the Southern Ocean since the 1990s has prevented the weakening of its carbon sink by trapping the upwelled carbon-rich deep water in the subsurface. The enhanced density stratification has prevented these CO_2-enriched waters from reaching the surface, and, thus hindered a saturation of the carbon sink in this period. Meanwhile, the surface layer became thinner, allowing the CO_2-rich circumpolar deep water to get closer to the surface, replacing winter water between 100 and 200 m. In this layer, the CO_2 fugacity increased by ~ 10 µatm since the 1990s. Consequently, our findings imply that the model-predicted weakening of the Southern Ocean carbon sink has been delayed by the surface freshening and might emerge when the stratification weakens.

Main

The Southern Ocean, south of 35°S, accounts for ~ 40% of the global oceanic uptake of anthropogenic carbon dioxide (CO_2)[1–4]. Thus, it removes a disproportionally large share of anthropogenic CO_2 from the atmosphere, making it a key ocean region for the mitigation of climate change[3]. The efficiency of this CO_2-sink is inherently linked to the Southern Ocean overturning circulation that allows exchanges of heat and carbon between the deep ocean and the surface[5,6]. As much as 80% of the global ocean's deep water returns to the surface in this region[7], carrying large amounts of dissolved inorganic carbon (DIC) accumulated globally in the deep ocean over centuries[8]. This return pathway through the Southern Ocean is visible as a circumpolar band of high-CO_2 waters at the subsurface[9], reaching the surface south of the Antarctic Circumpolar Current, where it induces a CO_2 release to the atmosphere and controls the amount of anthropogenic CO_2 entering the surface ocean while these waters are transported northward[10].

Previous studies suggested that an increased Southern Ocean overturning circulation due to human-induced climate change would profoundly weaken the future carbon sink[11,12]. In these simulations, climate change and ozone depletion lead to a poleward intensification of westerly winds[13–15], associated with a more positive phase of the Southern Annular Mode (SAM)[16,17]. Subsequently, the increase in the wind-driven upwelling is expected to enhance the CO_2 outgassing of the Southern Ocean[18,19], and to limit its uptake capacity of anthropogenic CO_2. This effect has been shown in a large range of biogeochemical model's simulation[12], atmospheric inversions[11,20] and oceanic[21] observations, which reported a weakening of the sink into the mid-2000s. Similarly, simulations of future climate

consistently predict a trend toward stronger westerly winds[22,23] and an expected further weakening or stagnation of the Southern Ocean carbon sink[11].

On the contrary, observations of oceanic fugacity of CO_2 (fCO_2) evidenced a reinvigoration of the Southern Ocean carbon sink since the 2000s[24–26]. The mechanisms behind this strengthening remain a topic of active research[27], making the future evolution of this critical carbon sink highly uncertain. Atmospheric changes, such as regional wind variability, have been put forward to explain this trend[24,28]. However, these studies also emphasize the complexity of the Southern Ocean carbon sink, highlighting that its evolution cannot be explained by local atmospheric conditions alone. Another plausible, yet unproven, explanation is the role of an increased salinity-driven stratification of the near-surface waters[24,26,29,30]. Paleoclimate studies have linked stratification changes to shifts in carbon sink efficiency: During periods of increased stratification, deep-water masses become isolated from the atmosphere, reducing CO_2 release and potentially contributing to lower atmospheric CO_2 levels[31–33]. These insights from past climates provide valuable context for understanding how stratification dynamics might influence the Southern Ocean's carbon sink in the present and the future.

In this study, we conducted a circumpolar analysis of repeat transects of long-term carbonate biogeochemistry sampling in the Southern Ocean. By interpreting the changes along hydrographic lines repeated multiple times, we observed that the potential for CO_2 outgassing increased by on average 10 µatm in the subsurface (100–200 m) layer since the 1900s. An analysis of water masses for each hydrographic section reveals that the anomalies are due to circumpolar deep water reaching shallower depth (on average 40 m shallower), coherent with the predicted increase in upwelling driven by stronger westerly winds[34]. However, this anomaly remains confined to the subsurface due to a significant increase in stratification, which acts as a barrier to vertical mixing. Since the 1980s, a pronounced freshening of the Southern Ocean has been observed[35–37], which is confirmed by our analysis of a subset of data that also contains biogeochemical observations since the 1990s (see Methods). This surface freshening has strengthened the upper ocean’s density stratification, limiting the exchange of carbon between the surface and deep waters. The enhanced stratification prevents the subsurface CO_2 anomaly from reaching the surface, temporarily stalling an increase in CO_2 outgassing from the subsurface, which explains the observed strengthening of the Southern Ocean carbon sink in this period.

Circumpolar increase in subsurface fCO_2 since the 1990s

Since the 1990s the subsurface (about 100 to 200 m) fugacity of CO_2 (fCO_2), without the contribution of anthropogenic fCO_2, has consistently increased across all seven hydrographic sections of the Southern Ocean (south of 55°S) studied (Fig. 1). We here calculated fCO_2 from the observed dissolved inorganic carbon (DIC, adjusted to reflect changes in ocean circulation only; see Methods), total alkalinity (TA), salinity, and temperature. It shows an average subsurface (dashed box in Fig. 1.b) increase of 10.0 µatm across all sections (ranging from 2.4 µatm to 17.0 µatm) between the 1972 to 2013 climatology and the most recent sections (post-2013). The average subsurface fCO_2 increase ranges on average from 470 to

480 µatm, remaining well above current (2025) atmospheric levels (~ 420 µatm), which implies that these upwelling deep waters would lead to a CO_2 release at the surface.

Interestingly, these positive fCO_2 anomalies are of similar magnitude and consistently found across the seven regions, but only within a specific subsurface layer (dashed box in Fig. 1b). The value of $D_{ref,}$ the depth of the interface between two main water masses, varies by region; however, the consistent positive anomalies are always located between D_{ref} – 50 m and D_{ref} +100 m, roughly corresponding to depths between 100 m and 200 m. The consistency of these subsurface anomalies across a wide range of geographic regions suggests that they reflect a robust, large-scale long-term change. In contrast, closer to the surface (above D_{ref} – 50 m), the signal becomes more variable and the fCO_2 anomalies lack a distinct pattern (Fig. 1b). The top 100 m are most likely dominated by short-term processes, such as air-sea gas exchange, biological activity, and seasonal to interannual variability.

The subsurface increase in fCO_2 aligns with an intensification of the overturning circulation and indicates an increase in the CO_2 outgassing potential if this water mass would come in contact with the atmosphere. This increased outgassing potential south of 55°S would reduce the efficiency of the Southern Ocean CO_2 sink. However, as of the last repeat section in this dataset from the year 2019 (section I06S, Fig. 1b), surface and subsurface anomalies remain mostly decoupled. Thus, the positive signal appears not to have reached the surface in most sections and remains confined below 100 m. This decoupling between the subsurface and surface layers highlights the role of stratification in isolating these anomalies and stalling their propagation to the surface.

Upward displacement of deep water

The subsurface increase in CO_2 fugacity is directly linked to a change in water mass distribution over the past decades. In all seven sections analyzed, we observe that the upper Circumpolar Deep Water (uCDW) is replacing the Winter Water (WW) in the 100–200 m layer (Fig. 2). This transition results in a shallower uCDW layer, which is accompanied by an increase in the concentration of dissolved inorganic carbon (DIC) and a corresponding rise in fCO_2.

Each section reveals a shift in water mass properties between the 1972–2013 climatology and the recent (post-2013) measurements. The uCDW in the Atlantic sector, along the A12section (Fig. 3), is characterized by high DIC concentrations (~ 2260 µmol kg^{-1}, Fig. 3b & d), low oxygen levels (< 220 µmol kg^{-1}), and elevated salinity and temperature. Its fCO_2 is considerably higher than atmospheric levels (~ 570 µatm at depths greater than 500 m). In contrast, the WW is fresher (S < 34.5), colder (T < -1°C), and contains less DIC (~ 2210 µmol kg^{-1}). It is a younger water mass, formed through deep mixing in winter[38,39], resulting in higher oxygen concentrations (> 300 µmol kg^{-1}).

The recent sections since 2013 consistently show that the uCDW is reaching shallower depths compared to the 1990s (Fig. 2). The depth at which waters with fCO_2 higher than 500 µatm are present is

now shallower in these recent sections, matching the shallower occurrence of waters with oxygen levels below 215 µmol kg^{-1}. On average, the depth limit below which water contains an 80% uCDW fraction has become shallower by 40 m. This shoaling ranges from 17.6 m in section 6 to 83.3 m in section 5. This upward shift in uCDW, replacing WW, explains the positive fCO_2 anomalies observed at the subsurface.

In addition to this vertical redistribution, the properties of the source water masses have also evolved over time. The intermediate layer, between 90% WW and 90% uCDW, now exhibits properties more similar to uCDW, such as increased temperature and salinity, higher DIC levels, greater alkalinity, and lower oxygen concentrations (e.g., section A12; Fig. 3). However, this intermediate layer occupies a smaller volume, as it is progressively replaced by uCDW. Meanwhile, uCDW itself has become warmer (+ 0.2°C, in section A12; Fig. 3), in agreement with current literature[40,41], while WW has become colder (-0.17°C) and fresher (-0.06). The increasing density gradient between these water masses strengthens the density stratification in the upper water column (distance between curved isopycnals in Fig. 3c). The consistent changes across all seven sections (Fig. 2a) reflect a widespread alteration in water mass composition and biogeochemistry in the Southern Ocean over recent decades.

Near-surface freshening

While the uCDW is shoaling, the WW is freshening, further differentiating its properties from the underlying deep water. The observed freshening of the WW core (up to -0.3 in Section A12, Fig. 4) leads to an increase in stratification and prevents the uCDW from mixing with the WW. As a result, while the uCDW moves closer to the surface, leading to positive fCO_2 anomalies in the subsurface (Fig. 1), its direct exchange with the atmosphere is limited. Consequently, the freshening of the WW during this period prevented the outgassing associated with the upwelling of uCDW.

While temperature changes in the WW vary between sections, the freshening of WW is a consistent, circumpolar trend observed south of 55°S (all salinity sections in Extended Data Fig. 1), in agreement with previous observational and modeling studies[35,36,42]. This freshening impacts the physical and biogeochemical characteristics of the water column: the WW is becoming less alkaline (Fig. 3d) and more oxygenated (up to -50 µmol.kg^{-1} in section A12, Fig. 4), further increasing its biogeochemical distinction from the uCDW. Additionally, reduced WW density intensifies the stratification between WW and the shoaling uCDW. Long-term trends in uCDW, including increasing salinity and temperature (Fig. 3c), further reinforce this gradient, amplifying the contrast between these water masses.

Comparing the recent sections with the climatology therefore reveals a salinity anomaly dipole, where the WW is fresher, and the layer below is saltier as the WW is replaced by the uCDW (Fig. 4). While this cap currently mitigates surface outgassing, the ongoing shallowing of the uCDW and evolving properties of both water masses suggest that this balance may not persist indefinitely.

Conclusions

Our findings reveal that the enhanced freshening of the surface Southern Ocean caps an increased subsurface fCO_2 since the 1990s. This increase is linked to a vertical shift in water mass distribution, particularly due to the shoaling of uCDW. At the same time, stronger surface stratification has effectively isolated the high-CO_2 uCDW from the atmosphere, temporarily preventing outgassing. However, as stratification strengthens and uCDW moves closer to the surface, the subsurface layer between 100–200 meters is becoming warmer, more saline, and richer in DIC, indicating a higher potential for CO_2 outgassing if this water reached the surface. This shoaling of uCDW and the increased subsurface fCO_2 are consistent with an increased upwelling in the Southern Ocean due to stronger westerly winds in a changing climate[11–13]. However, we here show that uCDW and the high fCO_2 waters are being trapped at the subsurface and have thus not substantially reduced the surface CO2 uptake by the region as predicted by climate model simulations. This trapping is the result of an increased surface density stratification in this period.

As shown in prior studies[35,42] and supported here, the stratification of the Southern Ocean has been increasing due to a circumpolar decrease of surface salinity for several decades. This freshening is the result of an increased precipitation over evaporation in this region[43], an enhanced northward export of sea ice[44], and, possibly, an increased export of glacial melt from the continental shelf[36,45]. However, it remains difficult to predict the variability of the surface stratification of the Southern Ocean. In 2016, a strong change in sea-ice regime has been observed[46], as the period of growing sea-ice cover suddenly came to an end, and low sea-ice years are observed since then. This strong change in the sea-ice regime is suspected to arise from direct mixing between surface waters and uCDW[47]. As uCDW is relatively warm, it could efficiently melt sea ice or reduce sea-ice formation in the region. In particular, the low sea-ice extents in winter-time in the years 2023 and 2024 might be indicative of a stark erosion of the upper ocean stratification. However, currently there is no repeat sections in these years available with a good resolution of carbonate parameters. The biogeochemical implication of this transition would be more CO_2 outgassing as suggested by our results and in agreement with prior studies suggesting a weakening of the Southern Ocean carbon sink. As CO_2 would accumulate more in the upper ocean and, ultimately, the atmosphere, accelerating global warming.

Our analysis is limited to data collected primarily during the summer months, with only two post-2016 sections available (2018 and 2019). While we observe no significant changes in these recent sections, the surface signal in this well-stratified upper ocean during summer is often dominated by regional variability, and two sections are currently insufficient for drawing robust long-term conclusions if the upper ocean layer has already changed since the sea-ice decline. These limitations underscore the need for long-term biogeochemical time-series to disentangle decadal variability from climate change-driven responses.

Our results align with paleoclimate studies, which suggest that lower atmospheric CO_2 levels are expected when deep-water masses are isolated from the atmosphere[31,32]. This agreement highlights the importance of stratification changes in controlling carbon cycling in the Southern Ocean. Further

research is essential to fully understand the mechanisms and feedbacks at play and to predict how ongoing climate change might alter this balance. By isolating the subsurface signal arising from ocean circulation changes, we provide evidence of how changes in ocean dynamics and stratification can both mask and drive considerable shifts in the ocean's carbon cycle, having important consequences on the evolution of the Southern Ocean carbon sink with climate change.

Methods

Long-term biogeochemical anomalies. This study is based on the analysis of two versions of the Global Ocean Data Analysis Project (GLODAP) database. The 2023 version 2 of the data product[48] entails 1108 cruises with quality controlled biogeochemical measurements covering the global ocean from 1972 to 2021. For the Southern Ocean, we identified sections that were sampled at least twice between 1972 and 2013, and with at least one additional post-2013 sampling (except for section S04I in 2013). The post-2013 cruises are here referred to as 'most-recent cruises' (Extended Data Table 1), and data are vertically linearly interpolated over 33 depths levels for homogeneity with the climatology. They are then compared to the climatology in the second version of the GLODAPv2 database[49] that we use in this study, by selecting the closest grid point of the climatology for each vertical profile and taking the difference, which results in the computed anomalies. The 1972 to 2013 climatology is published on a 1° by 1° grid, and on 33 depths levels. The climatology along the sections identified is representative of an average over the 1980s to 2000s as several cruises were conducted during this time period. For simplicity, we refer to the climatology period as the "1990s" throughout the paper. The salinity, temperature, oxygen, Dissolved Inorganic Carbon (DIC) and Total Alkalinity (TA) anomalies are therefore the difference between the 1972 to 2013 climatology extracted along the identified repeated sections and the post-2013 sections. Physical parameters such as salinity and temperature from GLODAP are used to ensure the accuracy of the comparison between physical and biogeochemical parameters as recommended by the database guidelines[49].

Water mass identification. Due to the local water mass properties of the regions in which each section is located, water masses are defined from the Temperature-Salinity (TS) diagram (Fig. 3a) of each section (supplementary Table 1). Winter Water (WW) is located at the respective temperature and salinity minimum of the diagram (blue shaded area in Fig. 3a). The core of the upper Circumpolar Deep Water (uCDW) is located at the local temperature and salinity maximum (purple shaded area in Fig. 3a), deeper points than this subsurface temperature maximum are not considered in the analysis. The T-S thresholds defining the water masses are identified from the climatological values. They constitute the 100% WW and uCDW, respectively. To assess the water mass fraction, we orthogonally project the TS diagram points onto the WW-uCDW mixing line. Data points with distances (H, Extended Data Fig. 2) in T-S space greater than 0.25 from the mixing line are excluded from the analysis, as they likely reflect mixing between surface waters and uCDW rather than the target water masses. This threshold value is consistently applied across all sections analyzed in this study. Changing this value does not change the result significantly as long as not too many points from the surface waters are included in the analysis.

DIC from circulation. The DIC anomalies are strongly impacted by the anthropogenic increase of CO_2 in the ocean. In this study, the focus is on the impact of long-term changes in circulation patterns on water mass properties that are related to exchanges between subsurface and deep water masses, but not with the atmosphere. Therefore, we used TA as a tracer for mixing between the two water masses. We assume that the changes in TA (ΔTA) can be approximated by the climatological TA of the uCDW ($TA_{uCDWclim}$) multiplied by a mixing ratio (M_{ratio}), as mixing with uCDW is the main source of TA change. This mixing ratio can therefore be computed as: $M_{ratio} = \Delta TA / TA_{uCDWclim}$. We are interested in the DIC resulting from the same mixing process (DIC_m), therefore we define $\Delta DIC_m = DIC_{uCDWclim} \cdot M_{ratio}$, and $DIC_m = DIC_{clim} + \Delta DIC_m$.

Subsurface fCO_2 . The CO_2 fugacity in the subsurface is derived with the Matlab CO2SYS v3.1[50] software from TA and DIC_m. We here use potential temperature and surface pressure to compute a potential fCO_2, meaning the fCO_2 values that the water parcel would obtain if it was brought up to the surface. The nutrients required for the fCO_2 calculation are provided by the GLODAP database, and dissociation constants were taken as the one of Luecker et al. (2000)[51].

Declarations

Acknowledgements L.O. is supported by the Initiative and Networking Fund of the Helmholtz Association (VH-NG-19-33). F.A.H is supported by the European Union (ERC, VERTEXSO, 101041743) and the Initiative and Networking Fund of the Helmholtz Association (VH-NG-19-33). We acknowledge the efforts of the GLODAP community in producing a uniformly calibrated and quality-controlled dataset of carbonate system and other biogeochemical variables. In part, data were collected and made publicly available by the International Global Ship-based Hydrographic Investigations Program (GO-SHIP; http://www.go-ship.org/) and the national programs that contribute to it. We also extend our gratitude to the early data collection as part of the World Ocean Circulation Experiment (WOCE) and all other data collectors and contributors that maintain the Southern Ocean sections for many decades, as well as the associated reference and best practice groups for their invaluable work. A special thank you to Mario Hoppema and Olaf Boebel for maintaining the Prime Meridian section as part of the Hybrid Antarctic Float Observing System (HAFOS), for the associated data collection, and for their advice.

Author Contributions This study was conceptualized by L.O and F.A.H. L.O. wrote manuscript with substantial input from F.A.H. Both authors contributed to the interpretation of the results and review of the manuscript. Funding for this project was provided by F.A.H.

Code and Data Availability This study is based on GLODAP data, openly available[48,49]. All codes are available upon request.

Competing Interests The authors declare they have no competing financial interests. Correspondence and requests for materials should be addressed to L.O. (email: lea.olivier@awi.de).

References

1. Sabine, C. L. *et al.* The Oceanic Sink for Anthropogenic CO2. Science 305, 367–371 (2004).
2. Gruber, N. *et al.* The oceanic sink for anthropogenic CO2 from 1994 to 2007. Science 363, 1193–1199 (2019).
3. Frölicher, T. L. *et al.* Dominance of the Southern Ocean in Anthropogenic Carbon and Heat Uptake in CMIP5 Models. J. Clim. 28, 862–886 (2015).
4. Caldeira, K. & Duffy, P. B. The Role of the Southern Ocean in Uptake and Storage of Anthropogenic Carbon Dioxide. Science 287, 620–622 (2000).
5. Morrison, A. K., Waugh, D. W., Hogg, A. M., Jones, D. C. & Abernathey, R. P. Ventilation of the Southern Ocean Pycnocline. Annu. Rev. Mar. Sci. 14, 405–430 (2022).
6. Marshall, J. & Speer, K. Closure of the meridional overturning circulation through Southern Ocean upwelling. Nat. Geosci. 5, 171–180 (2012).
7. Talley, L. Closure of the Global Overturning Circulation Through the Indian, Pacific, and Southern Oceans: Schematics and Transports. Oceanography 26, 80–97 (2013).
8. Murnane, R. J., Sarmiento, J. L. & Le Quéré, C. Spatial distribution of air-sea CO2 fluxes and the interhemispheric transport of carbon by the oceans. Glob. Biogeochem. Cycles 13, 287–305 (1999).
9. Chen, H., Haumann, F. A., Talley, L. D., Johnson, K. S. & Sarmiento, J. L. The Deep Ocean's Carbon Exhaust. *Glob. Biogeochem. Cycles* 36, e2021GB007156 (2022).
10. Bushinsky, S. M. *et al.* Reassessing Southern Ocean Air-Sea CO2 Flux Estimates With the Addition of Biogeochemical Float Observations. Glob. Biogeochem. Cycles 33, 1370–1388 (2019).
11. Le Quéré, C. *et al.* Saturation of the Southern Ocean CO2 Sink Due to Recent Climate Change. Science 316, 1735–1738 (2007).
12. Lovenduski, N. S., Gruber, N. & Doney, S. C. Toward a mechanistic understanding of the decadal trends in the Southern Ocean carbon sink. Glob. Biogeochem. Cycles 22, (2008).
13. Waugh, D. W., Primeau, F., DeVries, T. & Holzer, M. Recent Changes in the Ventilation of the Southern Oceans. Science 339, 568–570 (2013).
14. Miller, R. L., Schmidt, G. A. & Shindell, D. T. Forced annular variations in the 20th century Intergovernmental Panel on Climate Change Fourth Assessment Report models. J. Geophys. Res. Atmospheres 111, (2006).
15. Gillett, N. P. & Thompson, D. W. J. Simulation of Recent Southern Hemisphere Climate Change. Science 302, 273–275 (2003).
16. Marshall, G. J. Trends in the Southern Annular Mode from Observations and Reanalyses. J. Clim. 16, 4134–4143 (2003).
17. Thompson, D. W. J. *et al.* Signatures of the Antarctic ozone hole in Southern Hemisphere surface climate change. Nat. Geosci. 4, 741–749 (2011).

18. Lovenduski, N. S., Gruber, N., Doney, S. C. & Lima, I. D. Enhanced CO2 outgassing in the Southern Ocean from a positive phase of the Southern Annular Mode. Glob. Biogeochem. Cycles 21, (2007).
19. Lenton, A. & Matear, R. J. Role of the Southern Annular Mode (SAM) in Southern Ocean CO2 uptake. Glob. Biogeochem. Cycles 21, (2007).
20. Lenton, A. *et al.* Sea–air CO_2 fluxes in the Southern Ocean for the period 1990–2009. *Biogeosciences* 10, 4037–4054 (2013).
21. Metzl, N. Decadal increase of oceanic carbon dioxide in Southern Indian Ocean surface waters (1991–2007). Deep Sea Res. Part II Top. Stud. Oceanogr. 56, 607–619 (2009).
22. Zheng, F., Li, J., Clark, R. T. & Nnamchi, H. C. Simulation and Projection of the Southern Hemisphere Annular Mode in CMIP5 Models. J. Clim. 26, 9860–9879 (2013).
23. Goyal, R., Sen Gupta, A., Jucker, M. & England, M. H. Historical and Projected Changes in the Southern Hemisphere Surface Westerlies. *Geophys. Res. Lett.* 48, e2020GL090849 (2021).
24. Landschützer, P. *et al.* The reinvigoration of the Southern Ocean carbon sink. Science 349, 1221–1224 (2015).
25. Gregor, L., Kok, S. & Monteiro, P. M. S. Interannual drivers of the seasonal cycle of CO2 in the Southern Ocean. (2018) doi:10.5194/bg-15-2361-2018.
26. Munro, D. R. *et al.* Recent evidence for a strengthening CO2 sink in the Southern Ocean from carbonate system measurements in the Drake Passage (2002–2015). Geophys. Res. Lett. 42, 7623–7630 (2015).
27. Gruber, N., Landschützer, P. & Lovenduski, N. S. The Variable Southern Ocean Carbon Sink. Annu. Rev. Mar. Sci. 11, 159–186 (2019).
28. Keppler, L. & Landschützer, P. Regional Wind Variability Modulates the Southern Ocean Carbon Sink. Sci. Rep. 9, 7384 (2019).
29. Lovenduski, N. S. & Ito, T. The future evolution of the Southern Ocean CO < SUB > 2</SUB > sink. J. Mar. Res. 67, 597–617 (2009).
30. Terhaar, J., Frölicher, T. L. & Joos, F. Southern Ocean anthropogenic carbon sink constrained by sea surface salinity. Sci. Adv. 7, eabd5964 (2021).
31. François, R. *et al.* Contribution of Southern Ocean surface-water stratification to low atmospheric CO2 concentrations during the last glacial period. Nature 389, 929–935 (1997).
32. Anderson, R. F. *et al.* Wind-Driven Upwelling in the Southern Ocean and the Deglacial Rise in Atmospheric CO2. Science 323, 1443–1448 (2009).
33. Hasenfratz, A. P. *et al.* The residence time of Southern Ocean surface waters and the 100,000-year ice age cycle. Science 363, 1080–1084 (2019).
34. Hogg, A. M., Spence, P., Saenko, O. A. & Downes, S. M. The Energetics of Southern Ocean Upwelling. J. Phys. Oceanogr. 47, 135–153 (2017).
35. Swart, N. C., Gille, S. T., Fyfe, J. C. & Gillett, N. P. Recent Southern Ocean warming and freshening driven by greenhouse gas emissions and ozone depletion. Nat. Geosci. 11, 836–841 (2018).

36. Haumann, F. A., Gruber, N. & Münnich, M. Sea-Ice Induced Southern Ocean Subsurface Warming and Surface Cooling in a Warming Climate. *AGU Adv.* 1, e2019AV000132 (2020).
37. Pörtner, H.-O. *et al.* The ocean and cryosphere in a changing climate. IPCC Spec. Rep. Ocean Cryosphere Chang. Clim. (2019).
38. Toole, J. M. Sea ice, winter convection, and the temperature minimum layer in the Southern Ocean. J. Geophys. Res. Oceans 86, 8037–8047 (1981).
39. Spira, T., Swart, S., Giddy, I. & du Plessis, M. The Observed Spatiotemporal Variability of Antarctic Winter Water. J. Geophys. Res. Oceans 129, e2024JC021017 (2024).
40. Zu, Y., Gao, L., Guo, G. & Fang, Y. Changes of Circumpolar Deep Water between 2006 and 2020 in the south-west Indian Ocean, East Antarctica. Deep Sea Res. Part II Top. Stud. Oceanogr. 197, 105043 (2022).
41. Schmidtko, S., Heywood, K. J., Thompson, A. F. & Aoki, S. Multidecadal warming of Antarctic waters. Science 346, 1227–1231 (2014).
42. Sallée, J.-B. *et al.* Summertime increases in upper-ocean stratification and mixed-layer depth. Nature 591, 592–598 (2021).
43. Akhoudas, C. H. *et al.* Isotopic evidence for an intensified hydrological cycle in the Indian sector of the Southern Ocean. Nat. Commun. 14, 2763 (2023).
44. Haumann, F. A., Gruber, N., Münnich, M., Frenger, I. & Kern, S. Sea-ice transport driving Southern Ocean salinity and its recent trends. Nature 537, 89–92 (2016).
45. Roach, L. A. *et al.* Winds and Meltwater Together Lead to Southern Ocean Surface Cooling and Sea Ice Expansion. Geophys. Res. Lett. 50, e2023GL105948 (2023).
46. Purich, A. & Doddridge, E. W. Record low Antarctic sea ice coverage indicates a new sea ice state. Commun. Earth Environ. 4, 1–9 (2023).
47. Spira, T. *et al.* Wind-triggered Antarctic sea ice decline preconditioned by thinning Winter Water. Preprint at https://doi.org/10.21203/rs.3.rs-5919587/v1 (2025).
48. Lauvset, S. K. *et al.* The annual update GLODAPv2.2023: the global interior ocean biogeochemical data product. Earth Syst. Sci. Data 16, 2047–2072 (2024).
49. Lauvset, S. K. *et al.* A new global interior ocean mapped climatology: the 1° × 1° GLODAP version 2. Earth Syst. Sci. Data 8, 325–340 (2016).
50. Sharp, J. D. *et al.* CO2SYSv3 for MATLAB. Zenodo https://doi.org/10.5281/zenodo.4023039 (2020).
51. Lueker, T. J., Dickson, A. G. & Keeling, C. D. Ocean *p*CO2 calculated from dissolved inorganic carbon, alkalinity, and equations for *K*1 and *K*2: validation based on laboratory measurements of CO2 in gas and seawater at equilibrium. Mar. Chem. 70, 105–119 (2000).

Figures

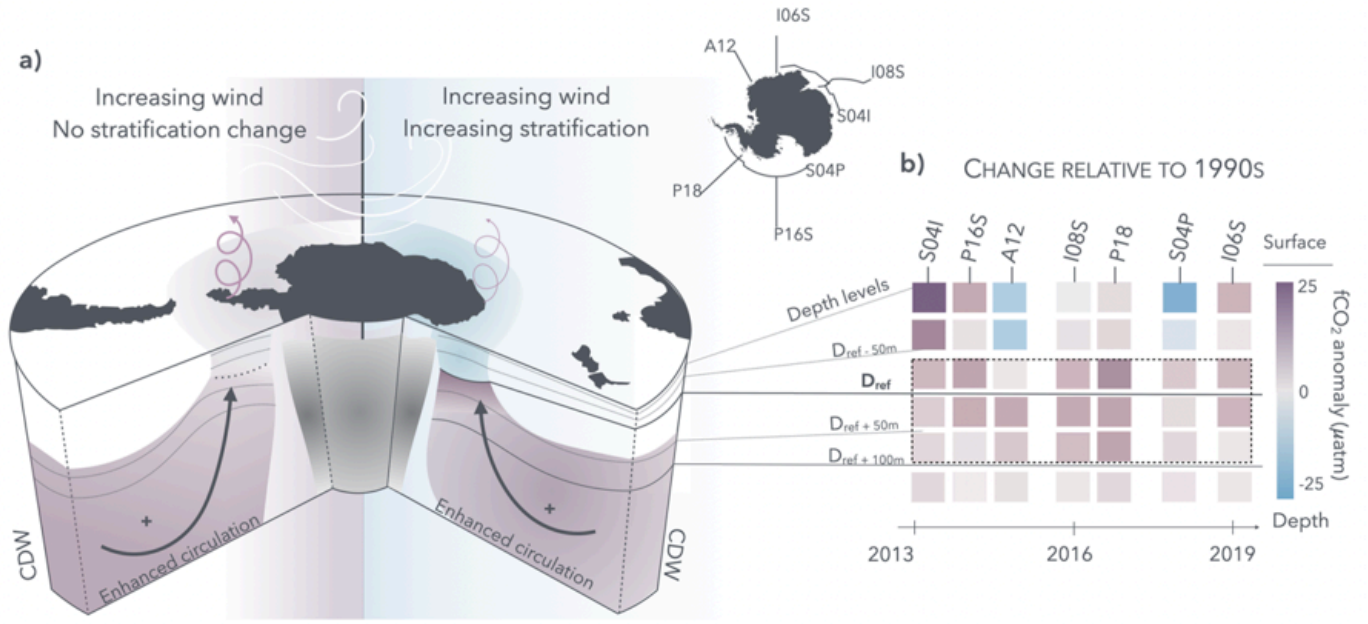

Figure 1

(a) Schematic of the effects of enhanced westerly winds (left) and, in addition, enhanced stratification (right) on the distribution of the water masses in the Southern Ocean. **(b)** Section-averaged fCO_2 anomaly (recent years minus climatology) calculated for depth layers across each section with anthropogenic carbon removed. The dashed box highlights the depth layers located in the subsurface. The inset map shows the location and names of the repeat sections analyzed in this study.

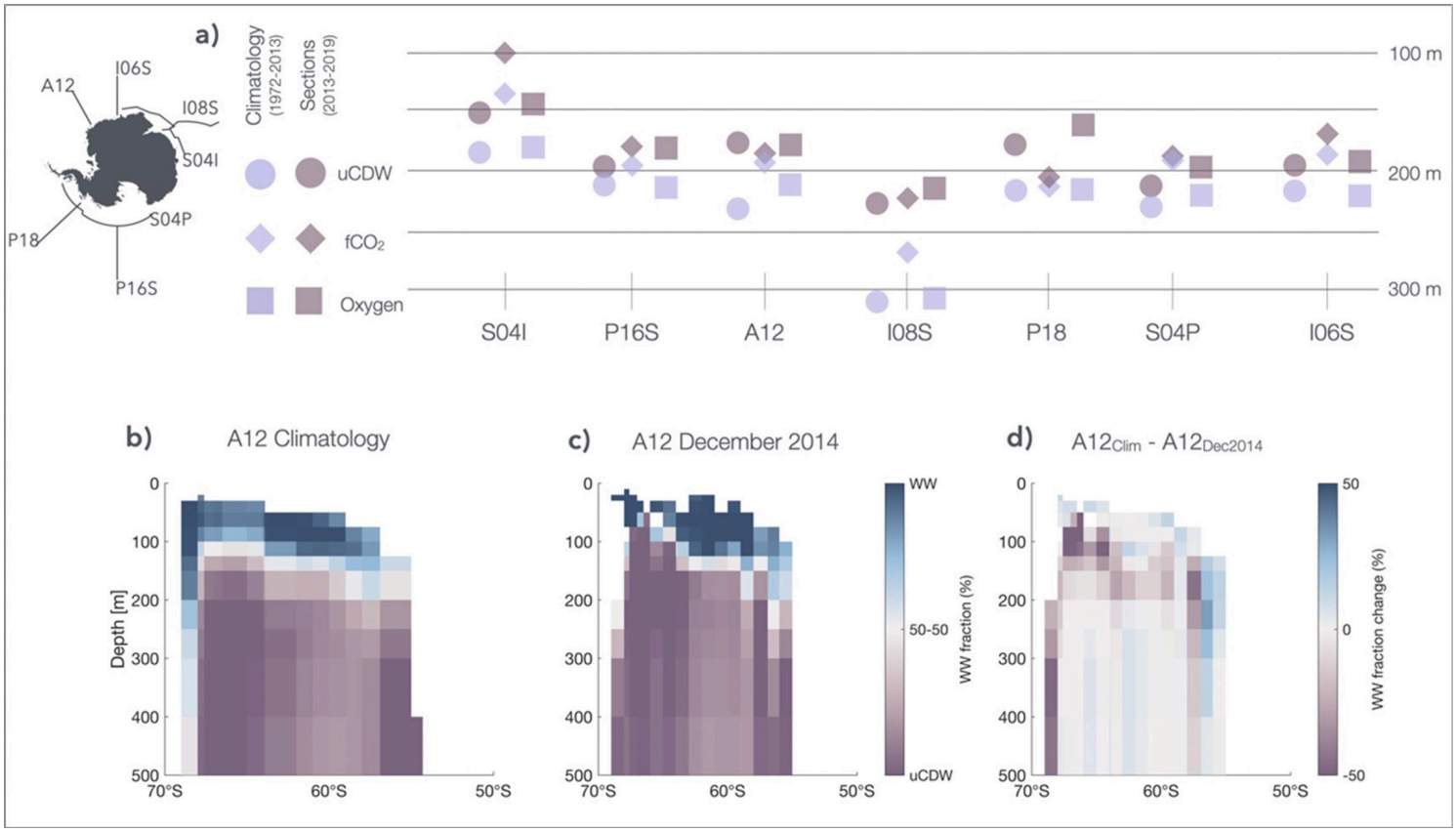

Figure 2

(a) Depth of the 80% upper Circumpolar Deep Water (uCDW) layer (circles), depth of the layer where fCO_2 exceeds 500 µatm (diamonds), and depth of the layer where oxygen levels fall below 215 µmol kg^{-1} (squares) for each section presented on the map. **(b)** Distribution of water masses along section A12 in the 1972–2013 climatology. **(c)** Distribution of water masses along section A12 in the most recent section (December 2014). **(d)** Changes in water mass distribution between the climatology and the December 2014 section.

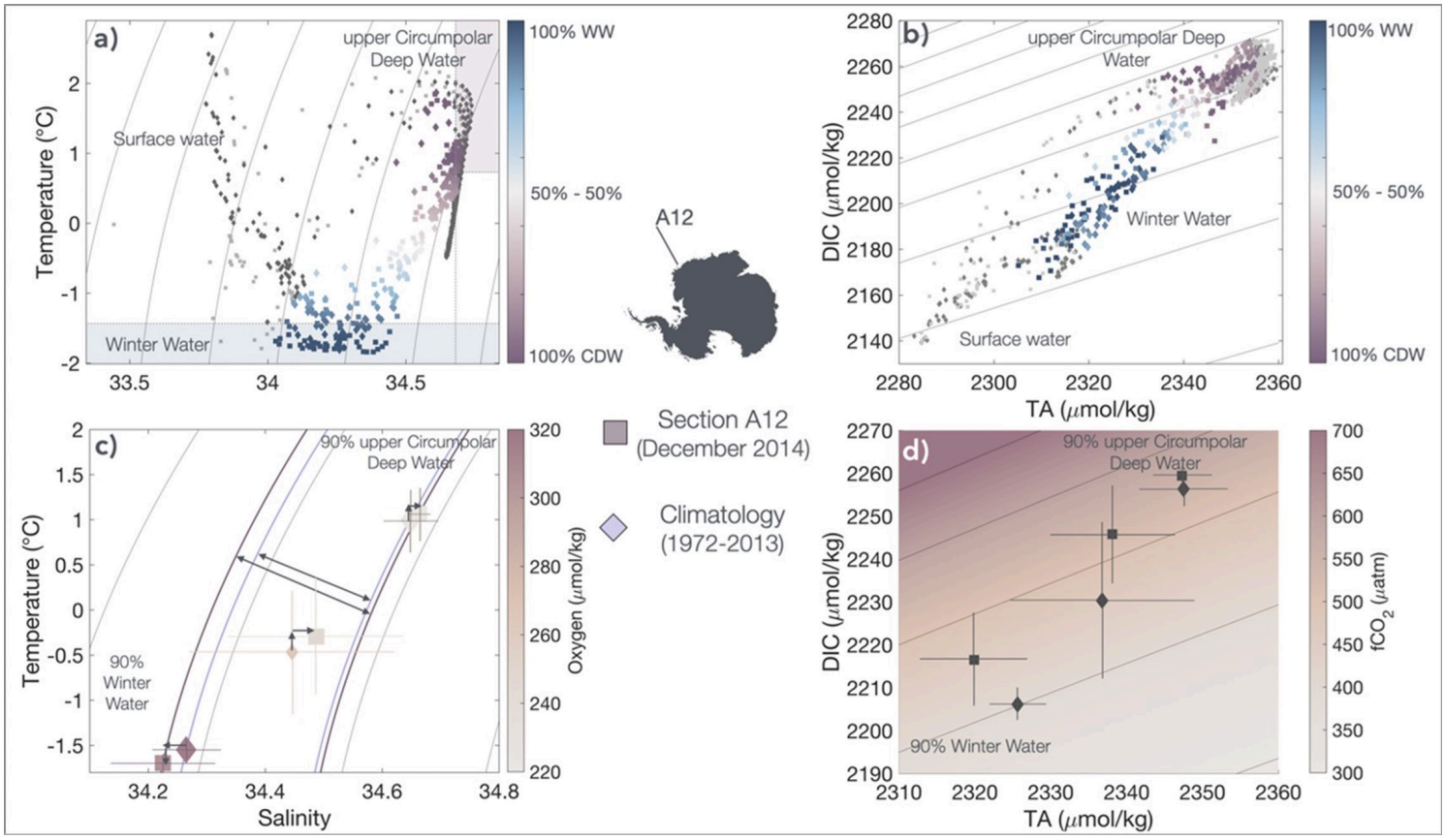

Figure 3

(a) Temperature-salinity (TS) diagram for section A12 in the 1972–2013 climatology (diamonds) and the most recent section (December 2014, squares), color-coded by water mass fraction. Shaded areas define 100% Winter Water (WW) and 100% upper Circumpolar Deep Water (uCDW) (see Methods). **(b)** Dissolved Inorganic Carbon (DIC) vs. Total Alkalinity (TA) diagram for section A12 in the 1972–2013 climatology (diamonds) and December 2014 (squares), color-coded by water mass fraction. **(c)** Averaged TS values for 90% uCDW, 90% WW, and the intermediate water mass (between 90% WW and 90% uCDW), color-coded by mean oxygen levels. Numerical values for the means and standard deviations are presented in Extended Data Table 1. **(d)** Averaged DIC vs. TA values for 90% uCDW, 90% WW, and the intermediate water mass, with background fCO_2.

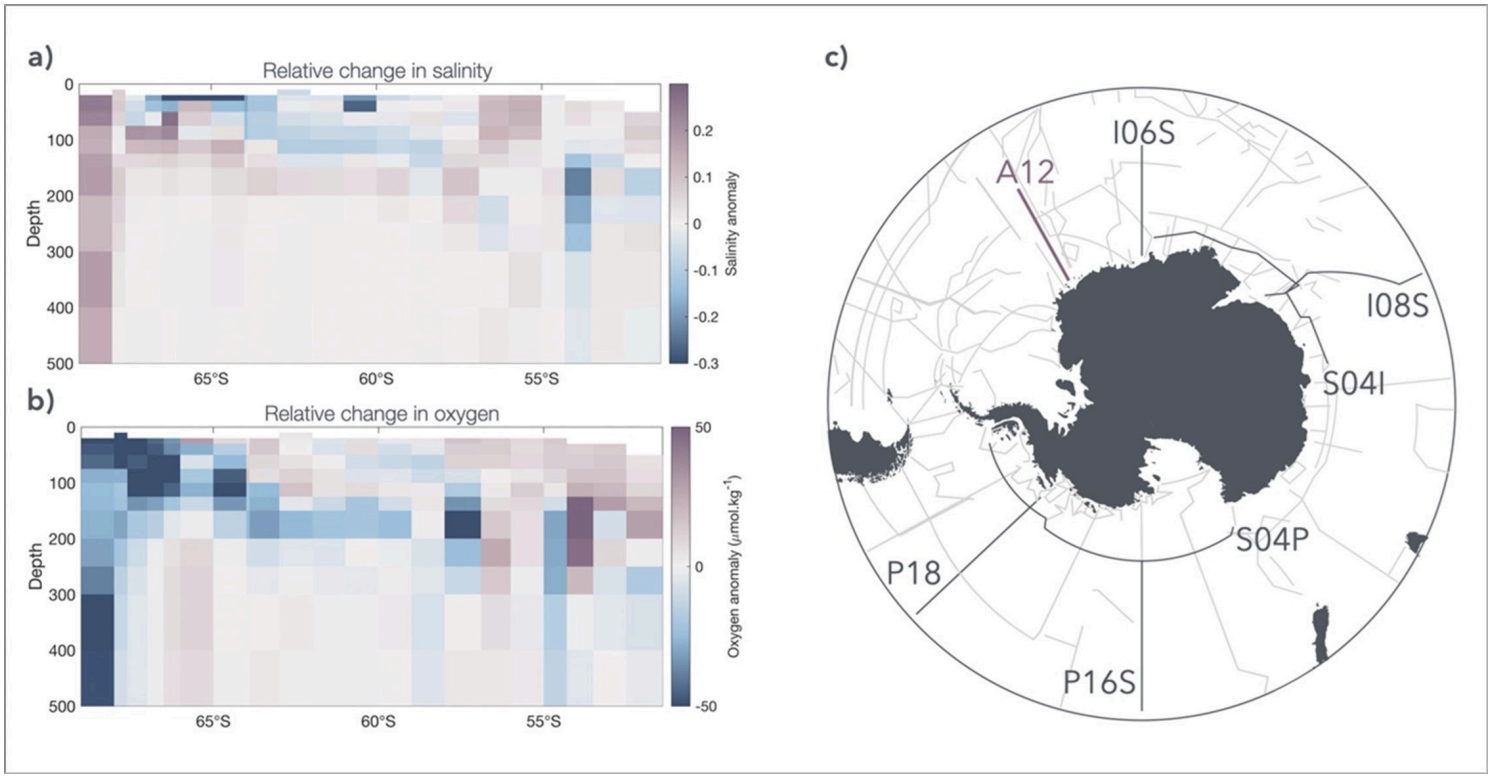

Figure 4

(a) Salinity anomalies between the 1972–2013 climatology and December 2014 along section A12. **(b)** Oxygen anomalies between the 1972–2013 climatology and December 2014 along section A12. **(c)** Map of all sections in the GLODAP database (light grey; see Methods) with repeat sections analyzed in this study highlighted (dark grey).

Supplementary Files

This is a list of supplementary files associated with this preprint. Click to download.

- ExtendedData.docx